Engineering and Laboratory Note Vol. 60, No. 22 / 1 August 2021 / Applied Optics 6573

applied optics

Optical transmittance of 3D printing materials

Shannon M. Hamp, Riley D. Logan, and Joseph A. Shaw*

Electrical and Computer Engineering Department and Optical Technology Center, Montana State University, P.O. Box 173515 Bozeman, Montana 59717-3515, USA

**Corresponding author: joseph.shaw@montana.edu*

Received 14 April 2021; revised 22 June 2021; accepted 26 June 2021; posted 28 June 2021 (Doc. ID 427525); published 28 July 2021

The increasing prevalence of three-dimensional (3D) printing of optical housings and mounts necessitates a better understanding of the optical properties of printing materials. This paper describes a method for using multi-thickness samples of 3D printing materials to measure transmittance spectra at wavelengths from 400 to 2400 nm [visible to short-wave infrared (IR)]. In this method, 3D samples with material thicknesses of 1, 2, 3, and 4 mm were positioned in front of a uniform light source with a spectrometer probe on the opposing side to measure the light transmittance. Transmission depended primarily on the thickness and color of the sample, and multiple scattering prevented the use of a simple exponential model to relate transmittance, extinction, and thickness. A Solidworks file and a 3D printer file are included with the paper to enable measurements of additional materials with the same method.

https://doi.org/10.1364/AO.427525

1. INTRODUCTION

3D printing technology is becoming widespread through engineering industries, including the field of optical engineering. Within this field, the applications of 3D printing range from 3D-printed optical elements [1–10] to 3D-printed mounts and enclosures [11–21]. In the fabrication of mounts and enclosures, it is critical to know how much light could be transmitted through the 3D-printed components. Even minimal transmission has the potential to elevate background signals and degrade the contrast of the measured signal for sensitive measurements.

The transmittance of 3D printing materials commonly used in optical mounts and enclosures could vary with wavelength, so spectrally resolved measurements are necessary. There are many examples of materials that are opaque in the visible spectrum while being partially transparent in one or more IR bands [22,23]. For applications covering a wavelength range beyond the visible spectrum, the possibility of transparency becomes concerning. The transmission properties of specific 3D components like light pipes [24] and lenses [25] have been compared to commercial products, and absorption and scattering coefficients have been reported for a white material and a gray material over the spectral range of 700–1000 nm [26]; however, the optical properties of a larger range of common printable plastics have yet to be evaluated from the visible through the shortwave IR (SWIR) spectral range, to the best of our knowledge. To begin filling this information gap, this paper presents measurements of transmission spectra for common 3D printer plastic filaments over the wavelength range of 400–2400 nm.

2. OPTICAL SETUP

Because the optical transmittance was expected to vary with the thickness and color of each of the 3D printing materials, samples were designed to allow for the measurement of multiple thicknesses, as shown in Fig. 1 (design files available online [27]). Each sample was printed from the same CAD file on a fused deposition modeling 3D printer (Creality Ender 5) and extruded with a 0.4 mm nozzle in the materials and colors presented in Table 1. We designed the sample so that four thicknesses of the material (1–4 mm) could be tested by shifting the sample sideways on a translation stage while changing nothing else in the setup for each measurement. The samples were also designed with a perimeter wall that, when lined with low-reflectivity paper (Edmund Optics Flock Paper #65), provided baffling around the measurement probe (although turning off the room lights made this shielding redundant). Note that the Flock paper is not so dark in the IR, so future users should consider more spectrally consistent dark materials [28].

The printed samples were mounted to an optical table on a linear translation stage for transmission measurements through each thickness without further adjustment of the setup. As shown in Fig. 2, the samples were positioned such that the spectrometer probe would remain 4 cm from the aperture of an integrating sphere that illuminated the sample with light from a halogen bulb. Note that an alternate approach could be to use a multiport integrating sphere configured to measure transmittance, although our setup only requires any bright light source that can fill the sample area with light that remains stable between the reference and sample measurements (1 min in our case). We have implemented this method using two different single-port integrating spheres (Sphere Optics unmarked model

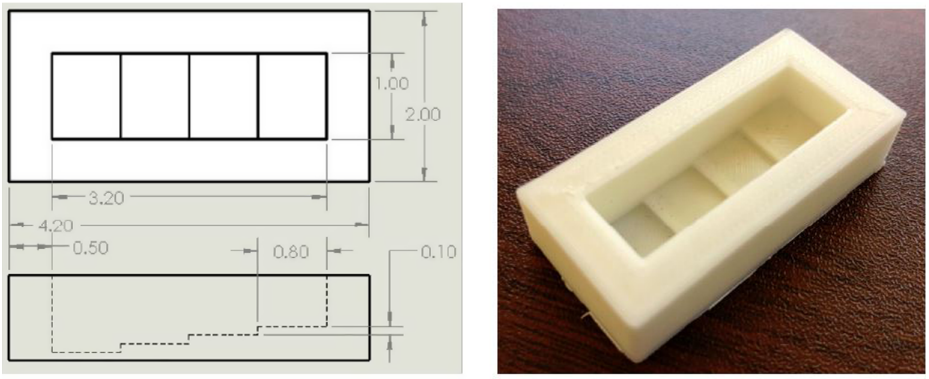

(a) (b)

Fig. 1. Sample design replicated for each material and color. (a) CAD drawing of sample design; (b) physical, printed sample.

Table 1. Measured Materials (All Printer Filament Had 1.75 mm Diameter)

Material	Color
Hatchbox acrylonitrile butadiene styrene (ABS)	Black
Hatchbox acrylonitrile butadiene styrene (ABS)	Gray
Coex Pro acrylonitrile butadiene styrene (ABS)	White
OVERTURE Nylon Filament (PA)	Black
Longsell polycarbonate material filament (PC)	Black
OVERTURE polyethylene terephthalate glycol (PETG)	Black
Hatchbox polylactic acid (PLA)	Black
Geeetech polylactic acid (PLA)	Blue
Hatchbox polylactic acid (PLA)	Gray
Novamaker polylactic acid (PLA)	White
Amazon Basics thermoplastic polyurethane (TPU)	Black

with 30 cm inner diameter and 12.5 cm aperture; Labsphere model V3ND-NNNN-NNSL-NS00-0000 with 30 cm inner diameter and 10 cm aperture). Transmission through each material sample was measured with a visible-SWIR spectrometer (Analytical Spectral Devices FieldSpec Pro). For each sample, the bare fiber spectrometer probe was positioned nearly flush with the largest step thickness so that the translation stage could be adjusted without disturbing the position of the probe between measurements. All measurements reported here were conducted in an interior laboratory space with all lights turned off to limit ambient light that could otherwise bias the measurement.

3. MEASUREMENT PROCEDURE

Measurements for each material type, color, and thickness were obtained from 400 to 2400 nm with 1 nm spectral resolution. Every measurement was taken with 136 ms integration time and averaged across 50 samples to increase the signal-to-noise ratio. To avoid saturating the reference measurements, the spectrometer was optimized to the integrating sphere source to determine the integration time of 136 ms. The integration time was then held at 136 ms so that all direct reference and sample measurements were directly comparable without linearity assumptions (to avoid saturating the reference spectra, we chose to adjust the exposure through the integration time alone while leaving the source brightness at maximum to limit any source spectral shifts). The reference measurement for black acrylonitrile butadiene styrene (ABS) is shown in Fig. 3, and the reference measurements for the remaining samples were visually indistinguishable from this curve.

To convert the raw digital number (DN) spectrum captured by the spectrometer to spectral transmittance, a direct reference measurement of the unobstructed integrating sphere aperture was recorded for each sample, maintaining the same spectrometer settings and physical position of the probe. The direct reference measurement for each sample was taken immediately

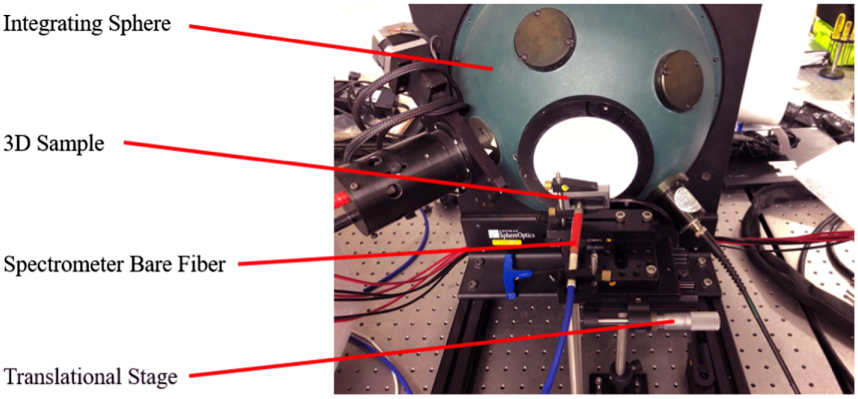

Fig. 2. Experimental setup showing sample placement, alignment of spectrometer fiber, linear translation stage, and integrating sphere.

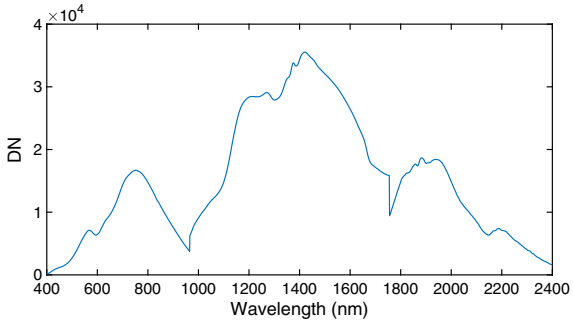

Fig. 3. Direct reference measurement associated with the black ABS sample. The reference measurements associated with the remaining 10 samples were visually indistinguishable from the above curve.

after the sample measurements so that <1 min elapsed between the measurements. The spectral transmittance of each material was calculated in 1 nm steps across the measurement range of 400–2400 nm as the ratio of light transmitted through the material sample (DN_{sample}) to the reference measurement from the unobstructed integrating sphere ($DN_{reference}$),

$$T = \frac{DN_{sample}}{DN_{reference}}. \quad (1)$$

The spectra were multiplied by 100 to obtain percent transmittance, shown in Figs. 4–6 for several 3D printing materials. As shown in Fig. 4, black materials [ABS, PA, polyethylene terephthalate glycol (PETG), and polylactic acid (PLA)] of 1 mm thickness exhibited an average transmittance of zero, with random noise ranging from approximately −1% to 1% in spectral regions with low detector sensitivity and lamp output. For both polycarbonate (PC) and thermoplastic polyurethane (TPU), transmittance rose in the IR to a peak near 2000 nm. However, when the thickness was increased to 2 mm, all black materials exhibited low and/or noisy signals, representing virtually zero measured transmission at all wavelengths.

In contrast to the spectral transmittance observed in black materials, colored samples of ABS and PLA exhibited greater spectral transmittance. Figure 5 presents the spectral transmittance of gray and white ABS. The gray sample exhibited a low signal and high levels of noise across the measured spectral range, again indicating effectively zero transmittance through the sample. Conversely, the white sample showed a relatively high maximum spectral transmittance of 19.0% at its greatest thickness of 4 mm. Figure 6 presents the spectral transmittance of blue, gray, and white PLA. For thicknesses greater than 1 mm, the spectral transmittance observed in the gray sample reduced to noise. However, the blue and white samples exhibited higher

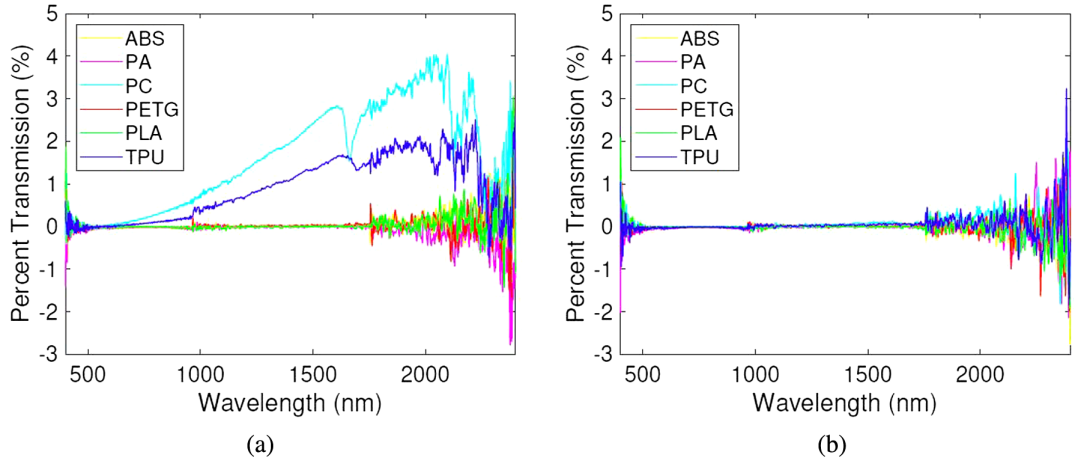

Fig. 4. Transmittance spectra of low-transmission, black materials. (a) Black filaments at 1 mm thickness; (b) black filaments at 2 mm thickness.

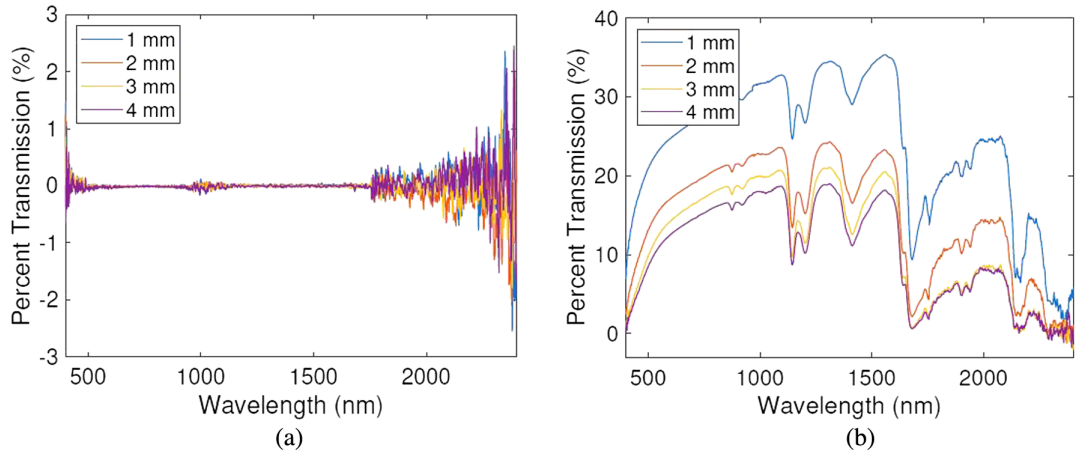

Fig. 5. Transmittance spectra of ABS at material thicknesses of 1–4 mm. (a) Gray ABS; (b) white ABS.

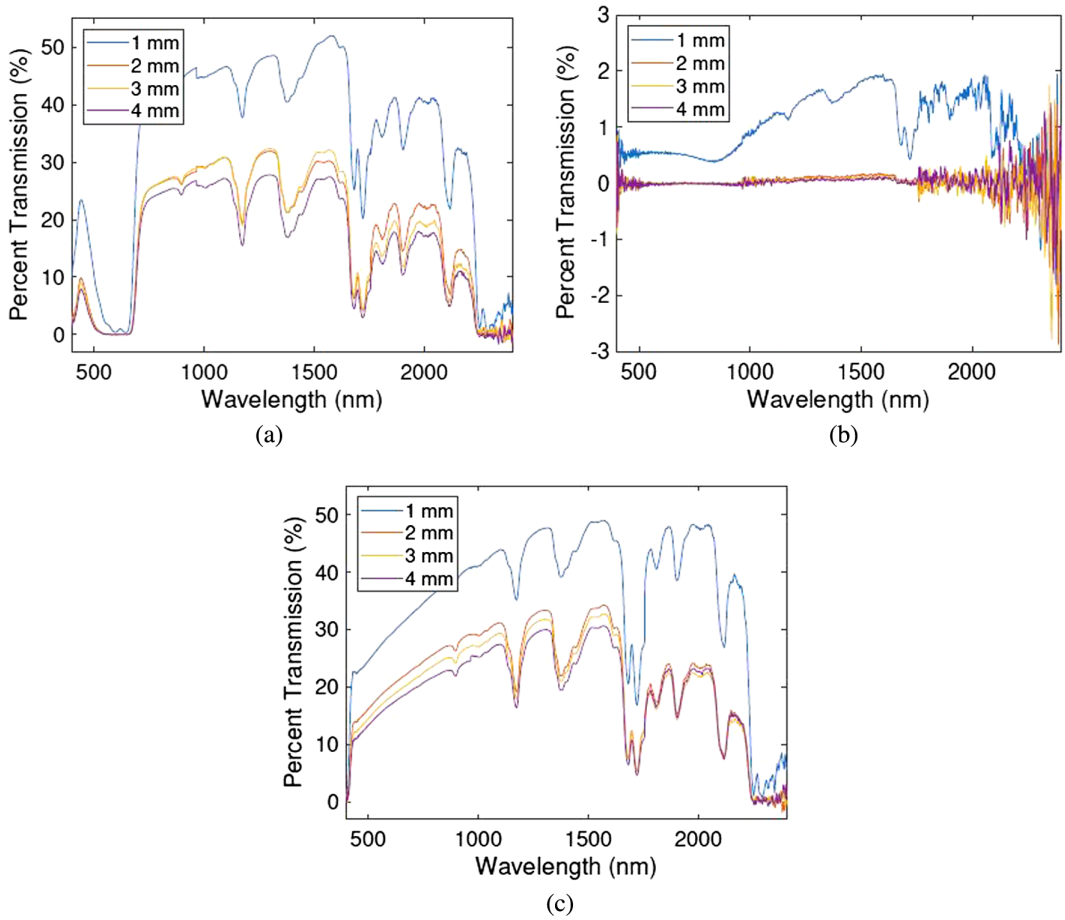

Fig. 6. Transmittance spectra of PLA at material thicknesses of 1–4 mm. (a) Blue PLA; (b) spectral transmittance of gray PLA; (c) white PLA.

spectral transmittance, with a relatively large maximum transmittance of 27.8% and 30.7%, respectively, at their greatest thickness of 4 mm. These results indicate that the spectral transmittance of the sample strongly varies with the color of the material, where lighter colors transmit greater percentages of light in comparison to absorptive colors like black. Nevertheless, PC and TPU are black materials that had notable transmittance over a wide spectral range.

The noise below 500 nm, near 1000 nm, and above 1750 nm in Figs. 4–6 when the sample transmittance was well below approximately 0.1% was caused by detector falloff and low lamp output (confirmed by the lack of noise in Fig. 3). The VIS-SWIR spectrometer uses three detectors to gather measurements across the spectral range of 400–2400 nm. The visible and near-IR spectrum (350–1050 nm) is measured by a 512-channel silicon photodiode, while the first SWIR spectrum (900–1850 nm) and second SWIR spectrum (1700–2500 nm) are measured by separate gallium arsenide detectors. Measurement uncertainty was highest in the spectral vicinity of these detector transitions, resulting in the most reliable measurements for 500–950 nm and 1050–1750 nm (on these regions the measurement uncertainty is less than 0.1%, and measurements are repeatable within this level).

The transmittance spectra can be used to calculate extinction coefficients α with a Beer–Lambert–Boguer law assumption of transmittance varying exponentially with the product of extinction coefficient and thickness. This leads to the following expression for extinction coefficient:

$$\alpha = \frac{-\ln(T)}{1\ \text{mm}}. \tag{2}$$

The extinction coefficients presented in Fig. 7 for the materials with reasonable transmittance through 1 mm thickness were obtained through Eq. 2. However, because the product of extinction coefficient and thickness is >1, the simple exponential model is not valid because multiple scattering dominates [29]. This can be confirmed by noting that the transmittance of white ABS at 1000 nm in Fig. 5 is approximately 0.31 for 1 mm thickness and 0.22 for 2 mm thickness. The former corresponds to extinction $= 1.17\ \text{mm}^{-1}$, while the latter corresponds to extinction $= 0.757\ \text{mm}^{-1}$, indicating that there is less light lost with the thicker sample than would be predicted by using the extinction coefficient derived with 1 mm thickness in an exponential model with 2 mm thickness. Therefore, in materials with significant multiple scattering, it is more accurate to measure the transmittance for a specific thickness rather than to use extinction, absorption, or scattering coefficients. Another option is to use a more complex scattering model, such as the doubling-adding method [26].

A related concern is that we see some evidence that multiple scattering could introduce a bias with the multithickness sample

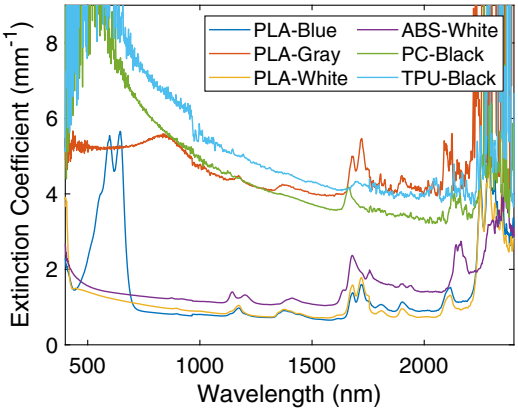

Fig. 7. Extinction coefficient plot for materials that demonstrated reasonable transmittance, from 1 mm thickness transmittance data.

relative to a fixed thickness. Therefore, the multithickness sample method is recommended for quick characterization of material transmittance, but a single-thickness sample would remove this uncertainty.

4. CONCLUSION

We presented a simple, easily replicated method for measuring spectral transmittance of common 3D printer filaments across a spectral range of 400–2400 nm for multiple material thicknesses and colors. The method uses a multithickness sample to enable measurements through different thicknesses without altering the setup. The multithickness measurements showed that multiple scattering requires transmittance to be measured for a desired thickness instead of assuming that transmittance is exponentially related to the extinction coefficient and thickness. The percent spectral transmittance data collected from the 3D printed material samples revealed that sample colors such as white, blue, and gray transmit light. In 1 mm thicknesses, the white ABS had a maximum transmittance of 35.4%, while the gray ABS exhibited a low signal. In 1 mm thicknesses of the PLA materials, the white, blue, and gray samples demonstrated a maximum transmittance of 49.0%, 52.0%, and 2.0%, respectively. However, all measured black samples (ABS, PA, PC, PETG, PLA, and TPU) demonstrated minimal spectral transmittance in sample thicknesses greater than 1 mm for all wavelengths in our spectral range. For the samples with 1 mm thickness, two of the black materials (PC and TPU) exhibited up to 4% transmittance in the SWIR. Our measurements demonstrate that the spectral transmittance of the sample varies with color and thickness of the material. Materials printed in thicknesses greater than 1 mm in absorptive colors, such as black, will transmit a negligible amount of light for most applications between 400 and 2400 nm, while deviations from these thicknesses and color selections will not reliably block light in the measured spectral range. A remaining uncertainty is how much the transmittance varies with different batches of material.

Funding. Air Force Research Laboratory; National Science Foundation EPSCoR (OIA-1757351); Montana State University Office of the Vice President for Research, Economic Development, and Graduate Education; Montana State University Undergraduate Scholars Program.

Acknowledgment. Thank you to the Makerspace at Montana State University for printing the 3D samples used in this work. S. Hamp thanks the Undergraduate Scholars Program and the Vice President for Research and Economic Development and Graduate Education for funding this research. J. Shaw and R. Logan thank the National Science Foundation EPSCoR Cooperative Agreement for support while this work was completed. Additionally, J. Shaw thanks the U.S. Air Force Research Laboratory through subcontract with S2 Corporation for support while this work was completed.

Disclosures. The authors declare no conflicts of interest.

Data Availability. Data underlying the results presented in this paper are available online: GitHub 3D Materials Testing Data.

REFERENCES

1. W. Kang, Z. Hong, and R. Liang, "3D printing optics with hybrid material," Appl. Opt. **60**, 1809–1813 (2021).
2. T. Grabe, Y. Li, H. Krauss, A. Wolf, J. Wu, C. Yao, Q. Wang, R. Lachmayer, and W. Ren, "Freeform optics design for Raman spectroscopy," Proc. SPIE **11287**, 34–43 (2020).
3. K. Weber, D. Werdehausen, P. König, S. Thiele, M. Schmid, M. Decker, P. W. D. Oliveira, A. Herkommer, and H. Giessen, "Tailored nanocomposites for 3D printed micro-optics," Opt. Mater. Express **10**, 2345–2355 (2020).
4. K. Weber, Z. Wang, S. Thiele, A. Herkommer, and H. Giessen, "Distortion-free multi-element hypergon wide-angle micro-objective obtained by femtosecond 3D printing," Opt. Lett. **45**, 2784–2787 (2020).
5. B. G. Assefa, M. Pekkarinen, H. Partanen, J. Biskop, J. Turunen, and J. Saarinen, "Imaging-quality 3D-printed centimeter-scale lens," Opt. Express **27**, 12630–12637 (2019).
6. B. G. Assefa, T. Saastamoinen, M. Pekkarinen, V. Nissinen, J. Biskop, M. Kuittinen, J. Turunen, and J. Saarinen, "Realizing freeform lenses using an optics 3D-printer for industrial based tailored irradiance distribution," OSA Contin. **2**, 690–702 (2019).
7. A. Toulouse, S. Thiele, H. Giessen, and A. M. Herkommer, "Alignment-free integration of apertures and nontransparent hulls into 3D-printed micro-optics," Opt. Lett. **43**, 5283–5286 (2018).
8. R. Saint, W. Evans, Y. Zhou, T. Barrett, T. M. Fromhold, E. Saleh, I. Maskery, C. Tuck, R. Wildman, F. Oručević, and P. Krüger, "3D-printed components for quantum devices," Sci. Rep. **8**, 8368 (2018).
9. J. Gawedzinski, M. E. Pawlowski, and T. S. Tkaczyk, "Quantitative evaluation of performance of three-dimensional printed lenses," Opt. Eng. **56**, 1–13 (2017).
10. J. Mici, B. Rothenberg, E. Brisson, S. Wicks, and D. M. Stubbs, "Optomechanical performance of 3D-printed mirrors with embedded cooling channels and substructures," Proc. SPIE **9573**, 30–43 (2015).
11. F. Kranert, J. Budde, P. Neef, R. Bernhard, M. Lammers, K. Rettschlag, T. Grabe, A. Wienke, J. Neumann, H. Wiche, V. Wesling, H. Ahlers, R. Lachmayer, and D. Kracht, "3D-printed, low-cost, lightweight optomechanics for a compact, low-power solid-state amplifier system," Proc. SPIE **11261**, 16–27 (2020).
12. R. Bogucki, M. Greggila, P. Mallory, J. Feng, K. Siman, B. Khakipoor, H. King, and A. W. Smith, "A 3D-printable dual beam spectrophotometer with multiplatform smartphone adaptor," J. Chem. Educ. **96**, 1527–1531 (2019).
13. M. Galvin, C. Delacroix, M. A. Limbach, T. Groff, M. Rizzo, and N. J. Kasdin, "Rapid-prototyping a tabletop integral field spectrograph," Proc. SPIE **11115**, 362–372 (2019).
14. I. Ferralli, T. Hordin, and M. Brunelle, "Leveraging 3D printing to streamline precision optical manufacturing," in *Optical Design and Fabrication 2019 (Freeform, OFT)* (Optical Society of America, 2019), paper OT3A.3.
15. I. A. Steele, H. Jermak, S. Bates, and I. Baker, "3D-printed optical instrumentation: practical starter designs and initial experiences," Proc. SPIE **10706**, 213–220 (2018).
16. M. Delmans and J. Haseloff, "μCube: a framework for 3D printable optomechanics," J. Open Hardware **2**, 1–9 (2018).

17. L. J. Salazar-Serrano, J. P. Torres, and A. Valencia, "A 3D printed toolbox for opto-mechanical components," PLOS ONE **12**, e0169832 (2017).
18. R. Stach, J. Haas, E. Tütüncü, S. Daboss, C. Kranz, and B. Mizaikoff, "polyhwg: 3D printed substrate-integrated hollow waveguides for mid-infrared gas sensing," ACS Sens. **2**, 1700–1705 (2017).
19. T. C. Wilkes, A. J. S. McGonigle, J. R. Willmott, T. D. Pering, and J. M. Cook, "Low-cost 3D printed 1 nm resolution smartphone sensor-based spectrometer: instrument design and application in ultraviolet spectroscopy," Opt. Lett. **42**, 4323–4326 (2017).
20. D. Myung, A. Jais, L. He, M. S. Blumenkranz, and R. T. Chang, "3D printed smartphone indirect lens adapter for rapid, high quality retinal imaging," J. Mobile Technol. Med. **3**, 9–15 (2014).
21. D. P. G. Nilsson, T. Dahlberg, and M. Andersson, "Step-by-step guide to 3D print motorized rotation mounts for optical applications," Appl. Opt. **60**, 3764–3771 (2021).
22. K. Mangold, J. A. Shaw, and M. Vollmer, "The physics of near-infrared photography," Eur. J. Phys. **34**, S51–S71 (2013).
23. J. K. Tong, X. Huang, S. V. Boriskina, J. Loomis, Y. Xu, and G. Chen, "Infrared-transparent visible-opaque fabrics for wearable personal thermal management," ACS Photon. **2**, 769–778 (2015).
24. K. Willis, E. Brockmeyer, S. Hudson, and I. Poupyrev, "Printed optics: 3D printing of embedded optical elements for interactive devices," in *Proceedings of the 25th Annual ACM Symposium on User Interface Software and Technology (UIST)* (Association for Computing Machinery, 2012), pp. 589–598.
25. H.-J. Kuo, C.-Y. Huang, W.-H. Wang, P.-H. Lin, H.-L. Tsay, and W.-Y. Hsu, "The study on surface characteristics of high transmission components by 3D printing technique," Proc. SPIE **10449**, 415–420 (2017).
26. Y. Liu, P. Ghassemi, A. Depkon, M. I. Iacono, J. Lin, G. Mendoza, J. Wang, Q. Tang, Y. Chen, and T. J. Pfefer, "Biomimetic 3D-printed neurovascular phantoms for near-infrared fluorescence imaging," Biomed. Opt. Express **9**, 2810–2824 (2018).
27. S. Hamp, "ORSL_3D_Materials_Testing," https://github.com/ShannonHamp/ORSL_3D_Materials_Testing.git, 2021.
28. J. L. Marshall, P. Williams, J.-P. Rheault, T. Prochaska, R. D. Allen, and D. L. DePoy, "Characterization of the reflectivity of various black materials," Proc. SPIE **9147**, 1459–1466 (2014).
29. C. Bohren and D. R. Huffman, *Absorption and Scattering of Light by Small Particles*, Wiley Science Paperback Series (Wiley, 2004).